SIMULATION OF SEMICONDUCTOR DEVICES AND PROCESSES Vol. 4
Edited by W. Fichtner, D. Aemmer - Zurich (Switzerland) September 12-14, 1991 - Hartung-Gorre

Numerical and Analytical Models of Selective Laser Annealing of Silicon-On-Insulator for 3-D Integration

A. Terao* and F. Van de Wiele
Laboratoire de Microélectronique, Université Catholique de Louvain
Place du Levant 3, B-1348 Louvain-la-Neuve, Belgium

Abstract

Both numerical and analytical models have been developped to simulate the thermal behaviour of an SOI substrate covered with anti-reflective and reflective stripes during a laser-induced zone-melting recrystallization process. The models are based on completely different sets of hypotheses and appear truely complementary. In particular, results obtained with the more flexible analytical model suggested how those given by the numerical one could be interpreted and exploited to gain maximum information.

The selective laser annealing introduced by J.-P. Colinge in 1982 [1] is still the only technique suitable for obtaining deposited layers of device-worthy monocrystalline silicon, and hence for three-dimensional integration. Although it has evolved since its invention, its principle has remained unchanged. A polysilicon layer is grown on top of an oxide covered wafer and then zone-melted with a scanning laser beam. A pattern of alternating anti-reflective (AR) and reflective (R) coatings deposited on the film modulates the power absorbed by the silicon and creates thermal gradients (Fig. 1).

The anti-reflective regions reach a higher temperature and thus recrystallize later than the neighbouring reflective regions. All crystalline defects concentrate at the middle of those regions, leaving the rest of the layer monocrystalline and defect-free. The optimization of this technique is very delicate, due to difficult control of numerous parameters : laser power, beam diameter, absorbance under AR and R coatings, substrate temperature, scanning velocity and direction, etc. Simulations could not replace all experimental studies but can help understanding the influence of each of those parameters on the thermal profile induced by the laser beam.

1 Numerical simulation

The complexity of the problem arises from its three-dimensional nature : the layers are stacked in one direction ($\vec{z}$), the anti-reflective and reflective stripes stretch into another ($\vec{y}$), and the laser beam is scanned along a third ($\vec{v}$). A three-dimensional numerical simulator would have been very bulky and computer time-consuming. So, only a 2-D simulator has been implemented, limited to a plane (xz) perpendicular to both the layered structure and the AR/R stripes. Moreover, the region under study was reduced to half a period λ of the stripe pattern, with periodicity and symmetry conditions at boundaries.

These hypotheses are strictly valid only at the middle of a stationary laser spot. A quasi-static assumption allows us to extend the applicability of the model to dynamical problems,

*Senior Research Assistant of the National Fund for Scientific Research, Belgium

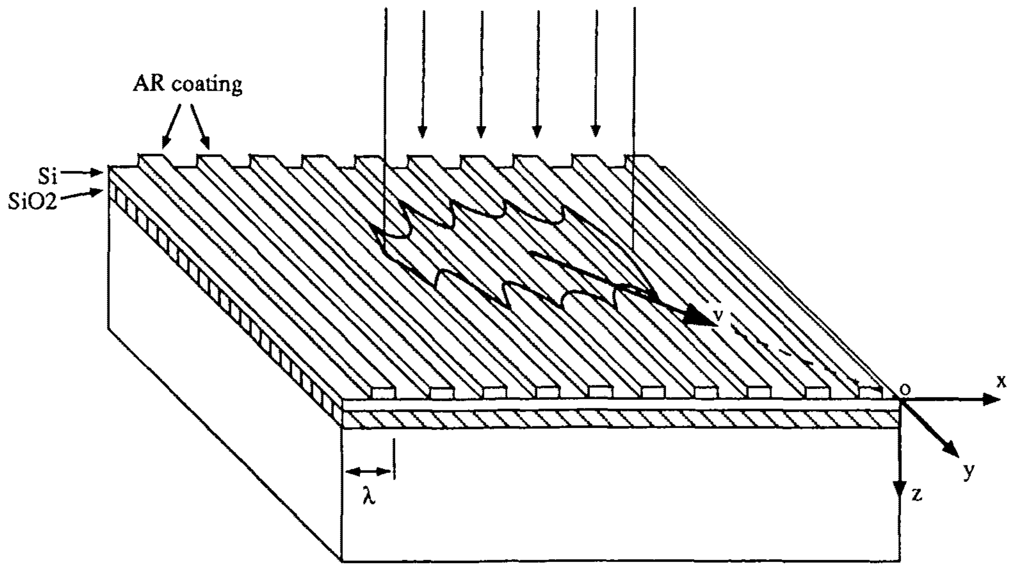

Figure 1: Principle of selective laser recrystallization

but the symmetry hypothesis will still limit the accuracy of this solution near the edge of the laser spot. In fact, almost all lateral heat flows are neglected, in both directions perpendicular and parallel to the plane of the model. There only remain an in-depth heat transmission and exchanges between adjacent AR and R regions.

The thermal equations were solved with a finite difference method, taking into account variations of optical and thermal coefficients with phase transitions. The equations are :

$$C_{p(\vec{r},T)} \frac{\partial T_{(\vec{r},t)}}{\partial t} = -\nabla \cdot \vec{J}_{(\vec{r},t)} + Q_{(\vec{r},t)} - H_{(\vec{r},T)} \tag{1}$$

$$\vec{J}_{(\vec{r},t)} = -\kappa_{p(\vec{r},T)} \nabla T_{(\vec{r},t)} \tag{2}$$

$C_{p(\vec{r},T)}$ $[J\,cm^{-3}K^{-1}]$ is the specific heat, $\vec{J}_{(\vec{r},t)}$ $[J\,s^{-1}cm^{-2}]$ is the heat flow, $Q_{(\vec{r},t)}$ $[J\,s^{-1}cm^{-3}]$ is the density of absorbed laser power, $H_{(\vec{r},T)}$ $[J\,s^{-1}cm^{-3}]$ is the heat generation rate for fusion and solidification, and $\kappa_{(\vec{r},T)}$ $[J\,s^{-1}cm^{-1}K^{-1}]$ is the thermal conductivity. The incident laser beam power is gaussian :

$$P_{(x,y,t)} = \frac{2}{\pi} \frac{P_0}{w^2} e^{-2\frac{(x-v_x t)^2+(y-v_y t)^2}{w^2}} \tag{3}$$

where P_0 $[W]$ is the total power of the beam, w $[cm]$ is its radius, and v_x and v_y $[cm\,s^{-1}]$ are the two components of the scan velocity. This power density is modulated by the AR/R stripe pattern and by the absorption profile in the multilayer structure :

$$Q_{(\vec{r},t)} = F_{(\frac{2\pi}{\lambda}x,z)} P_{(x,y,t)} \tag{4}$$

F does not depend on y as the stripes are kept parallel to that direction.

Starting from an equilibrium state with no laser power, i.e. $t \to -\infty$, the time variable was increased step by step. At each step, the 2-D system was solved with an ADI (Alternating Direction Iteration) method. When the scanning direction is parallel to the stripes, i.e. $v_x = 0$, the result, given as a function of time, can be reinterpreted to give the instantaneous temperature profile along a line in the same direction. This is done by establishing an equivalence between the coordinate y and the time t :

$$Q_{(x_0,y_0,z_0,t)} = F_{(\frac{2\pi}{\lambda}x_0,z_0)} \frac{2}{\pi}\frac{P_0}{w^2} e^{-2\frac{x_0^2+(y_0-v_y t)^2}{w^2}} \qquad \text{for } y_0 \text{ fixed and } t \text{ variable}$$

$$Q_{(x_0,y,z_0,t_0)} = F_{(\frac{2\pi}{\lambda}x_0,z_0)} \frac{2}{\pi}\frac{P_0}{w^2} e^{-2\frac{x_0^2+(y-v_y t_0)^2}{w^2}} \qquad \text{for } t_0 \text{ fixed and } y \text{ variable} \tag{5}$$

For all other scanning directions[1], this can not be done and much more computing is needed to determine the shape of the melted zone.

2 Analytical modelling

In order to complete this 2-D simulator, an analytical model has been developped, that takes account of the whole structure and 3-D heat flows. Of course, an analytical model could not pretend to be more general and accurate than a numerical one and a series of other approximations had to be made. The absorbed laser power was divided in two : a gaussian component Q_0 and a correction Q_p for the stripe pattern :

$$Q_{(x,y,z,t)} = Q_{0(x,y,z,t)} + Q_{p(x,y,z,t)} \tag{6}$$

Each component gives rise to a heat flow and thus two components of temperature can be computed. They were simply added, assuming a small magnitude for the perturbative term :

$$T_{(x,y,z,t)} = T_{0(x,y,z,t)} + T_{p(x,y,z,t)} \tag{7}$$

For the first term, a 3-D equation was solved only in the bulk silicon wafer, whereas a 1-D thermal flow was assumed in the thin surface layers of oxide and silicon. The 3-D part is based on an analysis given in reference [2]. The 1-D part is a simple integration of equations (1) and (2), with the quasi-static assumption ($\frac{\partial T}{\partial t} = 0$).

For the second term, the dependance in z was dropped and the heat flow was considered only in the plane of the silicon film, as there is no net flow toward the depth of the wafer and the silicon layer is thin compared to the width of the AR and R stripes [3]. Apart from a gaussian factor due to the laser beam profile, Q_p has a periodical crenel shape, with period λ. A Fourier decomposition can be applied :

$$Q_{p(x,y,t)} = \frac{2}{\pi}\frac{P_0}{w^2} e^{-2\frac{(x-v_x t)^2+(y-v_y t)^2}{w^2}} \sum_{n=1}^{\infty} q_n \cos\left(\frac{2\pi}{n\lambda}x\right) \tag{8}$$

Computations were limited to the first order term. With those hypotheses and at the expense of one numerical integration, it was possible to compute the instantaneous temperature profile under the moving laser beam with a separation of variables :

$$T_{p(x,y,t)} = T_{p1(y,t)} \cos\left(\frac{2\pi}{\lambda}x\right) + \cdots \tag{9}$$

This model is far easier to handle than the numerical simulation because all variables (x, y, and t) can be handled independently, and results can be rapidly presented in different forms : evolution of temperature at a given point, instantaneous thermal profile along a line, evolution of

[1] Actually, a similar manipulation can be done for a scan perpendicular to the stripes because $F(\frac{2\pi}{\lambda}x,y)$ is periodic.

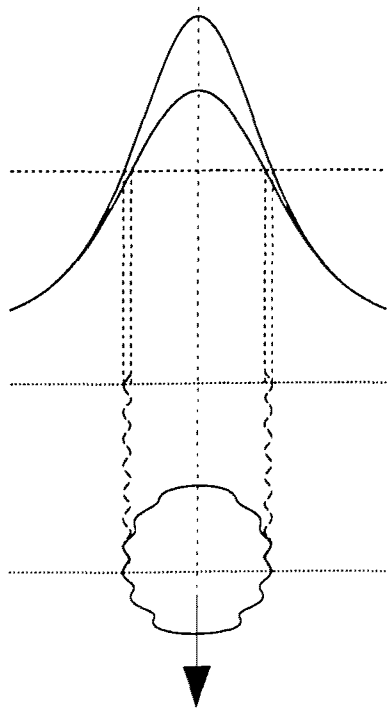

Figure 2: Some results obtained with the analytical model : 1-D thermal profiles at the centre of AR and R zones, and instantaneous 2-D isotherm

isotherms in the film plane (fig. 2). The latter is one of the most interesting, since the isotherm at the melting point of silicon can be considered to represent the liquid-solid interface. This is an approximation, since the analytical model can not account for any phase transition.

3 Discussion

The analytical model allowed to study the undulations of the edge of the melted zone for different positions of the laser spot relative to the AR/R stripes. To resume all situations, we computed two curves, named M_a and M_r, representing the locations of respectively the outward and the inward peaks of the melted zones (at the center of respectively the AR and R zones) for all positions of the stripes relative to the spot. For a fixed position, the edge of the melted zone (curve M) is confined between those curves (Fig. 3).

For a scanning parallel to the stripes, the pattern is stationnary, but for any slanted or perpendicular scan, the curve M glides between the curves M_a and M_r. An important conclusion is that the two curves M_a and M_r seem to be independant of the scanning direction. This is not obvious from the analytical expressions, but can be verified on numerical results. This suggests a way to extend the scope of the numerical simulations. As computations are much easier for a scan parallel to the stripe structure, the curves M_a and M_r can be determined for that configuration. Then, these curves are simply rotated for other scanning directions. An approximation of the shape of the melted zone can be obtained by alternately joining the points on the curves at the middle of AR and R zones. An a posteriori justification can be found assuming that the difference between AR and R zones is not too important, and that the size of the model is small enough. The region under study, wide as half the period λ and infinitely thin, can be considered as a tiny probe sensing the temperature both under AR and R stripes

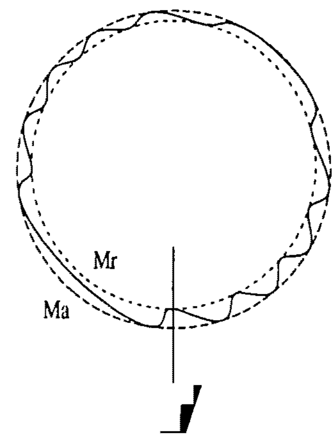

Figure 3: Curves M_a and M_r limiting the edge of the melted zone M for a slanted scan

at a given location. Only the mean position of this probe is important, its orientation has little influence. It is as if the temperature at the middle of AR and R zones were two independant functions evaluated at the same point.

A second important problem is the comparison with experimental results. Although the numerical simulation can give very accurate and detailled data, it is difficult to obtain corresponding experimental data because they are both microscopic and transient. The analytical model can be modified -in fact, simplified- to give the thermal profile only at the level of the center of the laser spot [3]. There, the temperature rise is near its highest and computed widths of the melted zone are maximum. This can be compared to the track left by a single scan across the stripes (fig. 3). Again transposing to the numerical model, we can obtain similar results, though with a less elegant trial-and-fail method. Using the preceding assumption, computations were of course carried out for a parallel scan and then transposed for slanted and perpendicular scans. The figure 4 shows a comparison between the three results. The fitting is reasonably good, considered that the models contain no adjustment parameter.

4 Conclusion

A physical model, whether numerical or analytical, is always a partial reflection of reality. We have shown here a case wherein two models, based on entirely different hypotheses and principles, could provide complementary results and lead to conclusions each one could not have revealed independently. The analytical model gives a three-dimensional, global point of view, and allows flexible manipulations by external computations. The numerical one is on the contrary cumbersome for automated handling, but gives a detailled description of a restricted region.

References

[1] J.-P. Colinge, E. Demoulin, D. Bensahel, and G. Auvert, "Use of Selective Annealing for Growing very Large Grain Silicon-On-Insulator Films," *Appl. Phys. Lett.*, 41(4), pp. 346-7 (15 Aug. 1982)

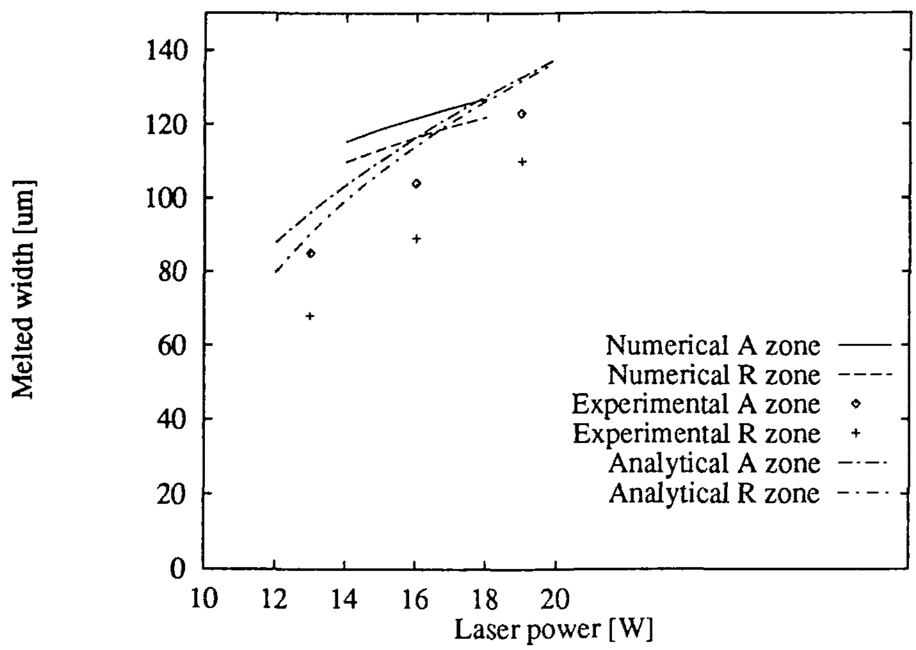

Figure 4: Comparison of experimental and simulated melted widths at the centre of AR and R stripes

[2] Y.I. Nissim, A. Lietoila, R.B. Gold, and J.F. Gibbons, "Temperature Distributions Produced in Semiconductors by a Scanning Elliptical or Circular cw Laser Beam," *J. Appl. Phys.*, 51(1), 274-279 (Jan. 1980)

[3] A. Terao, P. Paelinck, D. Flandre, P. Verlinden, and F. Van de Wiele, "Analytical Model for Selective Laser Annealing of SOI," *European SOI Workshop*, Meylan - France, p. A - 04 (March 1988)